



Advanced low blaze angle x-ray gratings via nanoimprint replication and plasma etch

DMITRIY L. VORONOV,^{1,2} SOOYEON PARK,^{1,3} ERIC M. GULLIKSON,¹
FARHAD SALMASSI,¹ AND HOWARD A. PADMORE¹

¹Lawrence Berkeley National Laboratory, 1 Cyclotron Road, Berkeley, CA 94720, USA

²dlvoronov@lbl.gov

³sooyeonpark@lbl.gov

Abstract: We developed a new method of making ultra-low blaze angle diffraction gratings for x-ray applications. The method is based on reduction of the blaze angle of a master grating by nanoimprint replication followed by a plasma etch. A master blazed grating with a relatively large blaze angle is fabricated by anisotropic wet etching of a Si single crystal substrate. The surface of the master grating is replicated by a polymer material on top of a quartz substrate by nanoimprinting. Then a second nanoimprinting is performed using the 1st replica as a mold to replicate the saw-tooth surface into a resist layer on top of a Si grating substrate. A reactive ion etch is used to transfer the grating grooves into the Si substrate. The plasma etch provides reduction of the groove depth by a factor defined by the ratio of the etch rates for the resist and Si. We demonstrate reduction of the blaze angle of a master grating by a factor of 5 during fabrication of a 200 lines/mm blazed grating with a blaze angle of 0.2°. We investigated the quality and performance of the fabricated low blaze angle gratings and evaluate process accuracy and reproducibility. The new blaze angle reduction method preserves the planarity of the optical surface of the grating substrate and at the same time provides improvement in the grating groove quality during the reduction process.

© 2023 Optica Publishing Group under the terms of the [Optica Open Access Publishing Agreement](#)

1. Introduction

High throughput of x-ray grating monochromators can be achieved at very small grazing angles especially when one wants to extend the operational energy range towards the tender or even hard x-ray region (i.e. above 2 keV). This applies to x-ray gratings with a low or medium groove density and extremely low blaze angles. For example, groove density as low as 50 lines/mm and a blaze angle of 0.12° are required for free electron laser (FEL) applications [1,2]. Blazed gratings with groove density of 240–305 lines/mm and the blaze angles of 0.27 -0.37° will be used in the monochromators of the new and upgraded beamlines of the Advanced Light Source-Upgrade (ALS-U) [3]. These low line densities still allow very high spectral resolution to be achieved, due to the extremely small angular size of the light source.

The diffraction efficiency of a blazed grating greatly depends on the shape of the grating grooves. It is challenging to make perfect saw-tooth grooves with blaze angles smaller than 1° by existing grating fabrication methods such as mechanical ruling [4], ion beam blasing [5], and anisotropic wet etching [6]. To address the problem, several methods for blaze angle reduction have been proposed. Saw-tooth grooves ruled in a layer of gold can be transferred into the Si substrate by Ar⁺ Ion Beam Etching (IBE) which provides a reduction of the groove profile owing to different sputter rates for gold and Si [7]. The reduction factor can be increased by adding oxygen ions which enables a chemical component to the IBE process. The saw-tooth shape of the grooves tends to degrade significantly during the ion etch transfer since highly energetic Ar⁺ ions tend to induce surface relaxation which results in smoothing of the grooves.

An alternative method of blaze angle reduction uses a low-power Reactive Ion Etch (RIE) applied to Si blazed gratings made by anisotropic wet etching [8]. The method is based on

planarization of a saw-tooth surface of a high blaze angle grating with a resist layer followed by RIE process to etch off the resist and underlying silicon material with slightly different etch rates, V_{resist} and V_{Si} respectively. (Figure 1(a)). The groove depth and the blaze angle reduce during the plasma etch by a reduction factor, R , which is defined by the etch rate ratio, V_{Si}/V_{resist} :

$$R = \frac{1}{1 - V_{Si}/V_{resist}} \quad (1)$$

The method is capable of providing blaze angle reduction by a factor of 10 and preserves the ideal shape of the grooves during the transfer process. Successful reduction of blaze angles down to the ultra-low value of 0.04° with high accuracy has been demonstrated [9]. However, practical use of the method for real x-ray gratings is problematic. A high reduction factor can be achieved only for an etch rate ratio close to 1, i.e. when the etch rate of Si is almost as high as the etch rate of the resist (see Eq. (1)). As a consequence of this, any imperfection of the top resist surface such as roughness, residual non-planarity, and resist thickness non-uniformity are fully transferred into the Si substrate. Those imperfections as well as non-uniformity of the plasma etch can significantly compromise the ultra-precise surface of the x-ray grating surface. For example, global non-uniformity of the resist layer thickness schematically shown in Fig. 1(b) will lead to unacceptable degradation of the initially plane surface of the grating substrate during the plasma etch. Since it is very challenging to achieve nanometer scale uniformity of the resist layer thickness and to control the plasma etch rate uniformity to the extent needed for massive rectangular grating substrates, this method is unreliable and has driven us to develop a method described here which is much more robust and insensitive to all kinds of process errors.

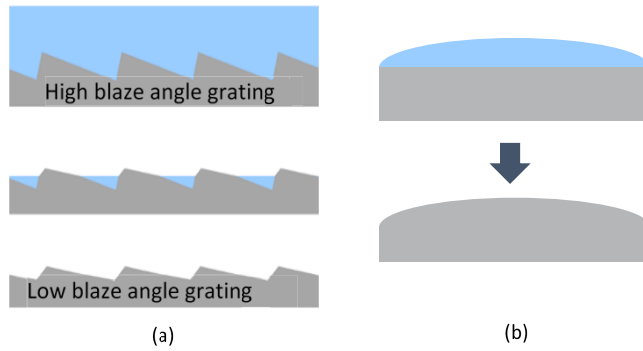


Fig. 1. Blaze angle reduction process via planarization and plasma etch: modification of the groove shape (a) and impact of process non-uniformity on the global shape of the optics (b).

In this work we propose a new approach for blaze angle reduction which preserves both a perfect saw-tooth groove shape and an ultra-precise surface of the x-ray optics (Fig. 2(a)). A master grating with a large blaze angle is replicated by a resist layer on top of the grating substrate by nanoimprint lithography (NIL). A following plasma etch provides transfer of the saw-tooth grooves into the Si substrate and a required reduction of the groove depth. A reduction factor for such a process is defined by the etch rate ratio:

$$R = \frac{V_{resist}}{V_{Si}} \quad (2)$$

To achieve a high reduction factor the etch rate of Si should be much smaller than the etch rate of the resist. As a result of this all possible imperfections of the resist surface and thickness non-uniformity will be scaled down by the reduction factor. The impact of the plasma etch

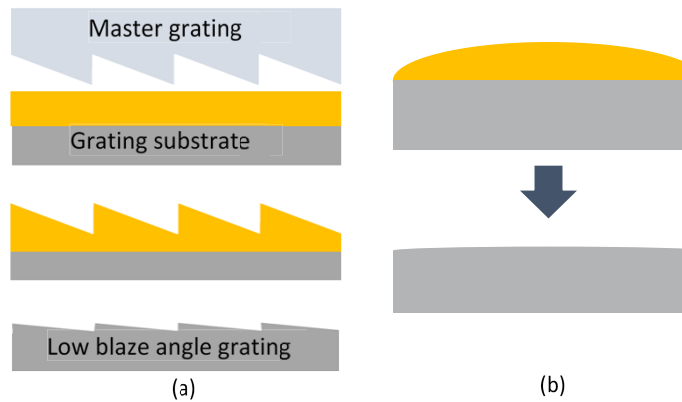


Fig. 2. Blaze angle reduction process via replication and plasma etch: modification of the groove shape (a) and reduced impact of process non-uniformity on the global shape of the optics (b).

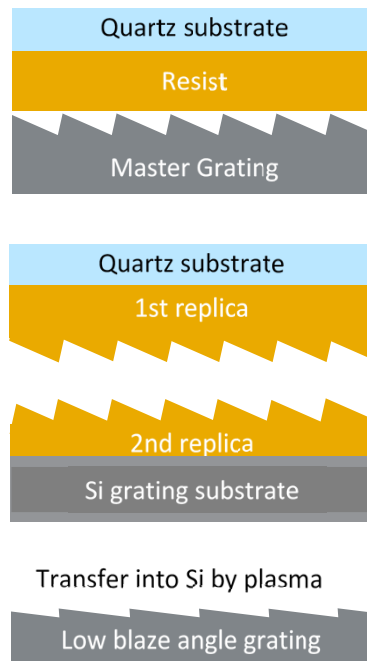


Fig. 3. Process flow for blaze angle reduction via double replication and plasma etch.

non-uniformity is also expected to be mitigated accordingly, so the final grating shape degradation should be negligible (Fig. 2(b)).

The replication process results in a flip of the blazed facet slope since the replica is a mirror image of the master grating (see Section 2.2(below)). This might not affect blazed gratings of constant groove density but is not acceptable for variable line spacing (VLS) gratings since the facet slope is coupled to the direction of the groove density variation. Moreover, in the case of using UV-curable resists, one of the NIL pieces, either a substrate or a mold, has to be transparent to UV light. To make a Si low blaze angle grating using a Si master grating, two cycles of the replication and plasma etch are required. First, the Si master grating is replicated and transferred

into a quartz substrate, and then the quartz saw-tooth surface is replicated and transferred into the Si grating substrate [10]. Such a multistep process increases the risk of surface degradation due to cumulative process errors. Moreover, the process requires expensive quartz substrates of high-quality surface finish, otherwise the quartz surface imperfections will be transferred into the final grating surface (with some scaling down). It is desirable therefore to reduce the number of the process steps and exclude the impact of the quartz surface on the replication process.

To address these challenges a new reduction process has been developed (Fig. 3). A high blaze angle master grating is first replicated by a resist material on a quartz plate using a NIL process. Then the resist replica is used as a mold to generate a second replica on a Si grating substrate. The resist grooves are transferred into the Si substrate by a single step of plasma etch providing the required groove depth reduction. Since the quartz surface is not directly involved in the transfer, the requirements for the quality of the quartz plates are significantly reduced.

In this work we report on fabrication of low blaze angle (LBA) gratings using the double-replication and plasma etch approach. We investigate the quality and performance of the gratings and evaluate reliability and reproducibility of the described fabrication method as well as capability to preserve the precision of the x-ray optics surface.

2. Experimental results

2.1. Master grating and LBA grating substrates

A 200 lines/mm master blazed grating was made by anisotropic wet etching of a single crystal Si substrate [11,12]. A custom orientation of the 100 mm × 40 mm × 18 mm substrate provided a tilt of Si (111) planes with respect to the substrate surface by a miscut angle of 1.8°. The substrate was polished flat down to $\lambda/20$ peak-to-valley (Fig. 5(a)). The grating pattern was transferred from a mask to the substrate by a lithography process [13]. Then a lift-off process was applied to create a hard mask composed of Cr stripes on the top surface of the substrate. An anisotropic wet etching with a 20 wt. % KOH solution was applied at room temperature for 2.5 hours to form the slanted facets of the grating. The saw-tooth grooves were finalized with wet isotropic etching.

A photograph and AFM images of the master grating are shown in Fig. 4. The saw-tooth grooves have somewhat curved facets (Fig. 4(b)) which is typical for anisotropically etched gratings [6], a groove depth of 100 nm, and an average slope of 1.1° of the blazed facets. Inspection of the grating with AFM revealed multiple pits on the faces surface (Fig. 4(c)). The pits are presumably caused by hidden defects of the crystal lattice such as dislocations, stacking faults etc. [14] left in sub-surface layer by the not-optimized polishing process. Etching of the defects results in pits and a rather high facet roughness of 1.6 nm rms. We chose this

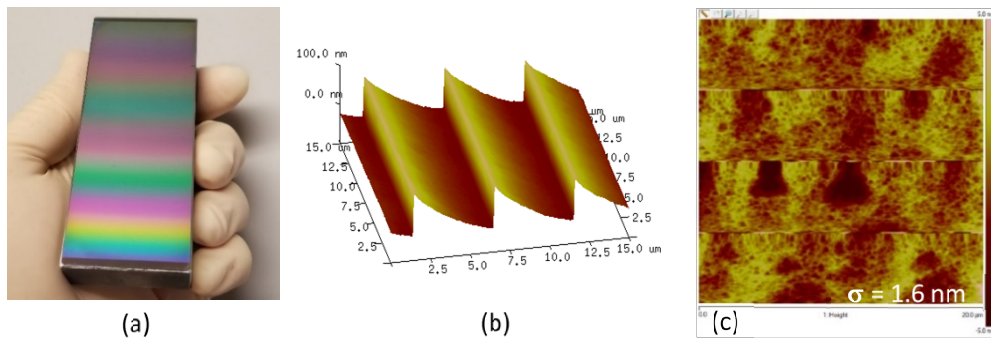


Fig. 4. A photograph (a) and AFM images (b, c) of the 100 mm × 40 mm × 18 mm Si master grating made by anisotropic etching.

quite low-quality blazed grating for this work to follow the evolution of the defects during the replication and reduction process.

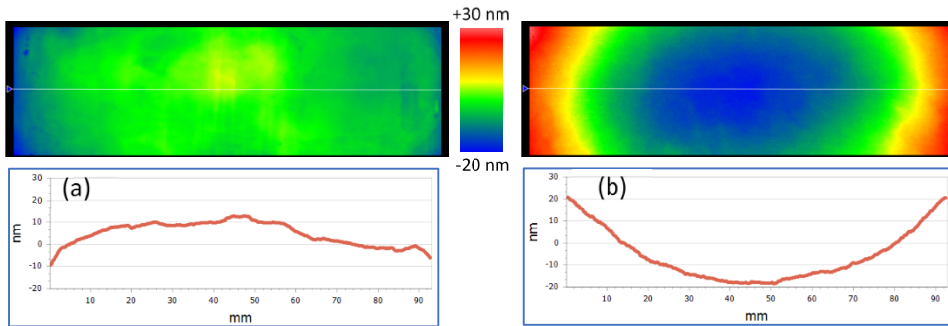


Fig. 5. Fizeau interferometer images of the master grating (a) and a low blaze angle grating substrate (b). The color scale corresponds to 50 nm height range.

Single crystal substrates for low blaze angle gratings with dimensions of $100\text{ mm} \times 40\text{ mm} \times 20\text{ mm}$ were made of Si (100) and polished flat down to $\lambda/10$ peak-to-valley flatness. A Fizeau interferometer image of a typical substrate is shown in Fig. 5(b). Although the surface precision of the substrates is insufficient for advanced x-ray optics, the substrates are good enough for investigation of the surface changes introduced by the grating fabrication process using Fizeau interferometry.

Quartz substrates of $100\text{ mm} \times 40\text{ mm} \times 6\text{ mm}$ for NIL replication were cut down from $6'' \times 6'' \times 0.25''$ semiconductor industry mask blanks with a surface flatness of $2\text{ }\mu\text{m}$.

2.2. Double replication of the master grating and plasma etch transfer

UV-curable resist mr-UVCur26SF from Microresist Technology GmbH [15] was used to replicate the master surface by NIL. The master grating was coated with a release layer and an adhesion promoter was applied to the quartz substrate. An air cushion nanoimprint setup [16] provided a pressure up to 90 psi on the master/substrate sandwich through flexible membranes in order to squeeze out the liquid resist down to a thickness of a few hundred nanometers. The resist was cured by UV flash exposure and then the pieces were separated. The resist replica on the quartz substrate was used as a mold for the 2nd NIL step to replicate the grooves on the Si grating substrate by a similar procedure. A photograph of the mold/substrate sandwich is shown in Fig. 6(a). Some color variations over the substrate area indicate that there is some non-uniformity of the resist layer thickness. The resist thickness on the grating substrate was measured by a Filmetrix optical spectrometer [17]. The 2D thickness map and 3D image of the resist surface are shown in Fig. 6(b) and 6(c). The measurements revealed a substantial non-uniformity of the resist thickness which varies from 180 to 260 nm over the substrate area. The resist thickness non-uniformity can be transferred into the silicon and compromise the substrate surface significantly but it is expected to be reduced during the plasma etch.

The groove profile for both replicas were inspected by AFM (Fig. 7). The nanoimprint process provides almost perfect replication of the saw-tooth grooves by the resist material. The 1st and 2nd replicas have convex and concave facets respectively. About 5% reduction of the replica groove depth occurs due to shrinkage of the nanoimprint resist during the curing. As a result of this, the resist grooves of the 2nd replica on the Si grating substrate are almost identical to the grooves of the master grating, but the groove depth has been reduced down to 90 nm.

The saw-tooth resist surface was transferred into the Si grating substrate by RIE plasma etch. The plasma etch recipe was developed to provide a reduction factor of 5.3 to achieve the goal blaze angle of 0.2° . We used a mixture of CHF_3 and O_2 gases with flow rates of 25 sccm and 3.1

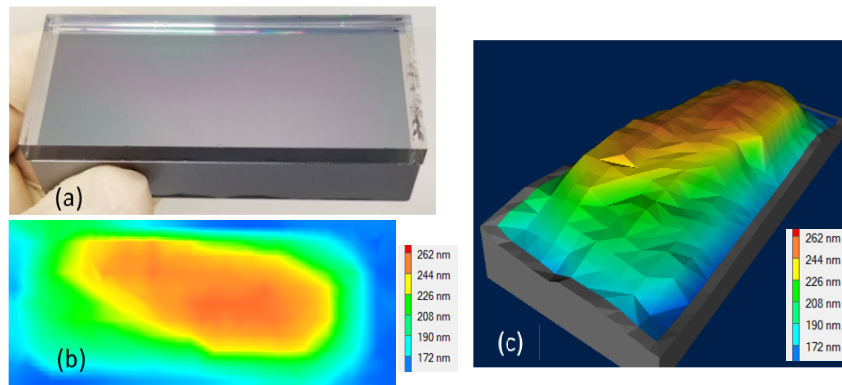


Fig. 6. A photograph of the substrate/mold sandwich (a), resist thickness map (b, c).

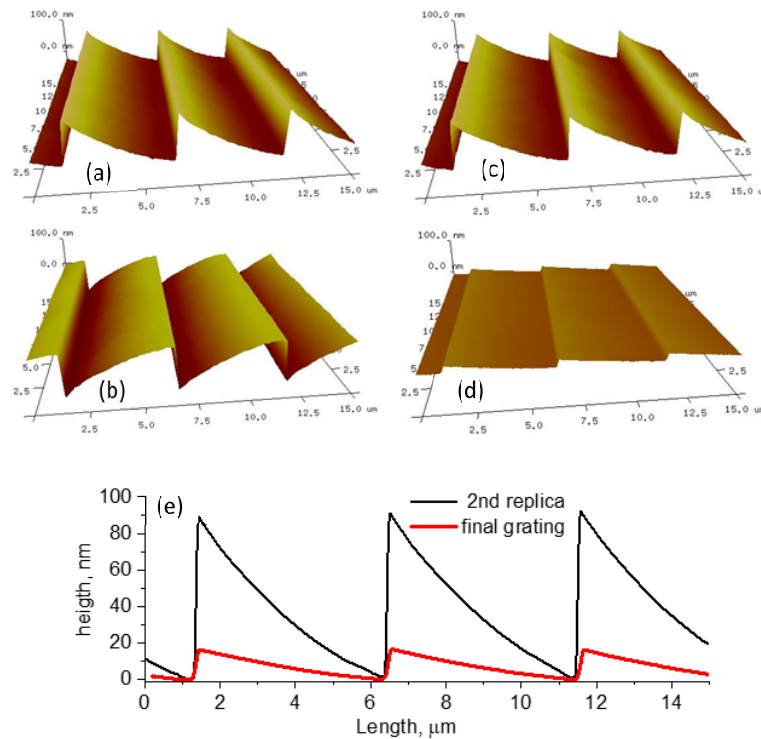


Fig. 7. AFM images of the master grating (a), 1st replica (b), 2nd replica (c), and the final low blaze angle grating (d), and profiles of the 2nd replica and the final grating (e).

sccm respectively. A plasma power of 30 W at a pressure of 30 mTorr provided etch rates of 15.8 nm/min and 3.0 nm/min for the resist and the Si respectively resulting in the goal etch rate ratio 5.3 : 1. An AFM image of the final low blazed grating after the 20-minute long plasma etch is shown in Fig. 7(d). The groove profiles of the grating before and after the plasma etch are shown in Fig. 7(e). The groove depth was reduced from 90 nm for the 2nd replica to 17 nm for the final grating and the facet curvature was reduced accordingly.

2.3. Surface roughness and figure errors

AFM images of the top surface of the final low blaze angle grating are shown in Fig. 8. The scans were performed along the grooves and then the images were line-by-line flattened to observe the surface morphology. The pits observed earlier on the facets of the master grating are mostly suppressed for the LBA grating, and a residual surface roughness of 0.45 nm rms was measured over scan areas of both $5\text{ }\mu\text{m} \times 5\text{ }\mu\text{m}$ and $20\text{ }\mu\text{m} \times 20\text{ }\mu\text{m}$. The high frequency roughness reduced by a factor of 3 compared to the master grating, which is somewhat smaller than the reduction factor of 5.3. The surface morphology indicates that some roughening of the resist surface occurred during the plasma etch, and the resist surface roughness was partially transferred into the facet surface. One can conclude that the LBA grating roughness is dominated by the resist roughening rather than the roughness of the master grating. To reduce further the grating surface roughness, one should find a resist which is more stable and preserves a smooth surface under the plasma etch conditions.

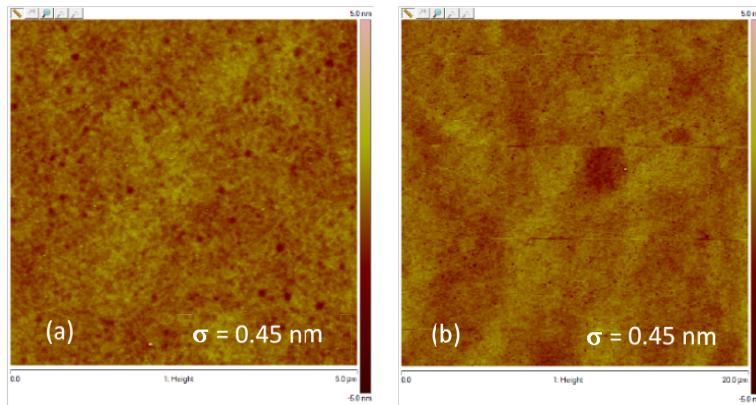


Fig. 8. Surface roughness of the final low blaze angle grating. The color scale bar corresponds to 10 nm.

A Fizeau interferometer image of the surface of the low-blaze angle grating is shown in Fig. 9(a). A differential map in Fig. 9(b) was obtained by subtraction of the original surface of the substrate shown in Fig. 5(b) from the final grating surface shown in Fig. 9(a). The differential map reflects a global change of the substrate shape during the fabrication process and shows the surface of the LBA grating assuming the ideally plane surface of the grating substrate. It is clearly seen that the differential map is very similar to the resist thickness map shown in Fig. 6(b), but scaled down by the reduction factor of around 5. The change of the grating surface and variation of resist thickness along the central line of the grating are shown in Fig. 9(c). We can conclude that the LBA surface errors are mainly caused by the non-uniformity of the nanoimprinting while the impact of the plasma etch non-uniformity seems to be minor. The reduction process greatly reduces the surface errors of the final LBA grating down to 10 nm p/v.

To investigate possible surface changes in the mid frequency range, the global shape was filtered out from the substrate surface before and after grating fabrication. The traces along the central line for the initial substrate and the final LBA grating perfectly coincide (Fig. 10) indicating that the blaze angle reduction process does not generate mid frequency surface errors. Summarizing this part, we can conclude that the fabrication process we developed introduces only minor errors in the global shape of the optics, it does not affect mid frequency features, and it suppress high frequency imperfections of a master grating.

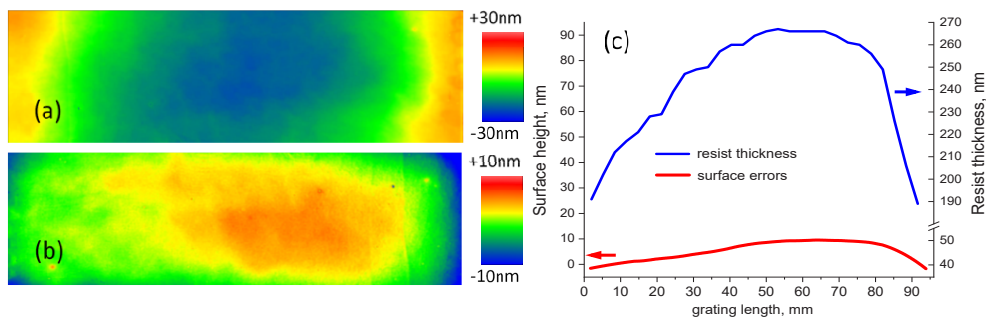


Fig. 9. Surface of the final low blaze angle grating (a), difference between the final and original surface of the grating (b), resist thickness variation (blue) and introduced surface errors (red) along the central line of the grating (c).

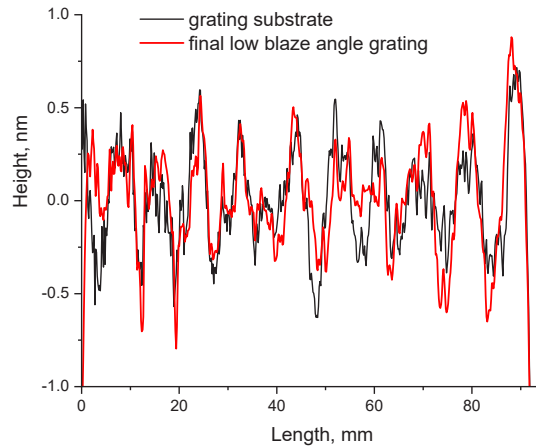


Fig. 10. Mid frequency surface variation of the original substrate surface (black) and final grating surface (red).

2.4. Accuracy and reliability of blaze angle reduction

To evaluate the accuracy, reliability, and reproducibility of the blaze angle reduction process we made 6 low blaze angle gratings using the same recipes. The profiles of the grooves of the LBA gratings are shown in Fig. 11(a). The average slope of the concave blazed facets is very close to the goal blaze angle of 0.2° for the gratings #4, #9, #11, and #13. The blaze angle of 0.187° measured for the grating #2 deviates from the goal by 7% which is well within the typical tolerance of 20% for low blaze angles. The blaze angle of 0.27° for grating #3 exceeds the goal value by 35% and might affect the grating performance, though still might be fine for many applications. One can conclude that 5 out of 6 gratings were made with high accuracy indicating the robustness of the process. Since the final blaze angle is defined by the plasma etch the reproducibility of the reduction process and accuracy of the low blaze angle can be enhanced by a careful calibration of the etch rates, plasma chamber conditioning etc.

The diffraction efficiency of the fabricated low blaze angle gratings was calculated in order to evaluate the impact of the groove imperfections on the grating performance. The efficiency simulations were performed using Rigorous Coupled Wave Analysis (RCWA) method using the RETICOLO package [18] for the constant included angle $2\theta = 174^\circ$. Minor deviation of the blaze angle from the optimal value results in a slight offset of the diffraction efficiency curves to higher or lower energies for the gratings #2, #9, #11, and #13 (Fig. 11(b)). The largest mismatch is

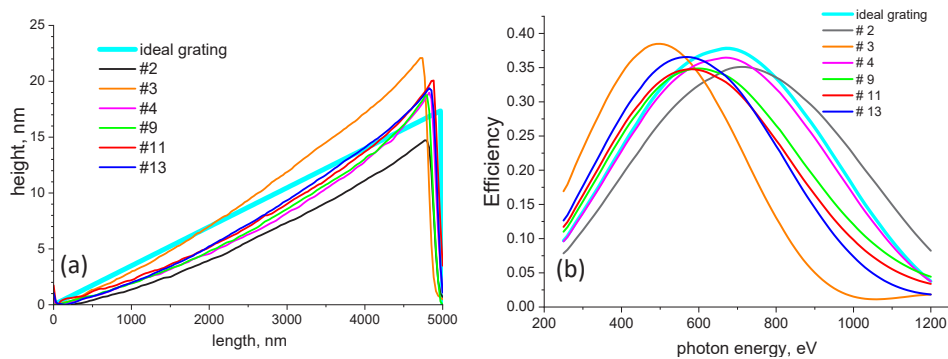


Fig. 11. Groove profiles (a) and efficiency simulations (b) for 6 low blaze angle grating fabricated by the same blaze angle reduction process.

observed for the grating #3 as expected. The efficiency curve of the grating #4 perfectly matches the theoretical diffraction efficiency.

Grating #4 was coated with gold and the diffraction efficiency was measured at beamline 6.3.2 [19] of the ALS. A 30 nm thick Au coating with a 5 nm thick Cr adhesive sub-layer was deposited by dc-magnetron sputtering using Ar sputtering gas. The efficiency measurements were performed at a constant included angle of 174° in the energy range of 250-1200 eV. The measured efficiency is in excellent agreement with simulation predictions (Fig. 12). A maximum efficiency of 35.8% was achieved for a photon energy of 650 eV, which is close to the theoretical efficiency of 37.6% for an ideal grating. The efficiency simulations performed for the real shape grooves show that the minor efficiency reduction is caused mostly by the residual facet curvature.

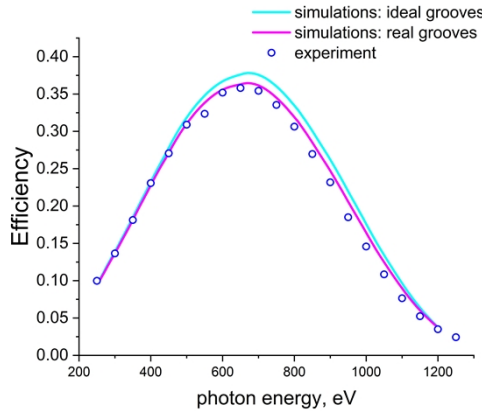


Fig. 12. Theoretical diffraction efficiency calculated for an ideal (cyan) and real (magenta) groove profile and experimental efficiency (blue circles) measured for the grating #4.

3. Discussion

The replication/reduction method we developed for making low blaze angle gratings provides a near perfect shape of the saw-tooth grooves required for high diffraction efficiency and at the same time preserves the highly precise optical surface of x-ray gratings. The method addresses the problem of the uniformity of large area nanoimprint, plasma etch etc., which is difficult to achieve for massive rectangular grating substrates. The impact of the process errors on the final grating quality is largely mitigated owing to the scaling down effect.

The method provides forgiveness for imperfections of a master grating and master grating substrates since the quality of the grating improves during the blaze angle reduction process. This simplifies master fabrication and significantly reduces the cost of expensive custom oriented Si (111) substrates required for anisotropic wet etching. It is challenging to achieve the ultra-precise optical surface of the substrate and precise custom orientation, and at the same time avoids hidden defects in the surface layer of the substrates, which cause pits during the wet etching and result in high surface roughness. The replication/reduction process offers solution for those problems since a whole set of the tight requirements can be split between the substrate for the master and a substrate for the final LBA grating. A master blazed grating with perfectly shaped grooves can be made using low-cost oriented substrates polished down $\lambda/10$ precision, while a final LBA grating will be done on widely available non-oriented Si (100) substrates with an ultra-precise optical surface. The surface imperfections of the master grating will be scaled down and the surface precision of the final LBA grating will be essentially the same as the surface of the ultra-precise Si (100) substrate.

Anisotropic wet etching provides near perfect saw-tooth grooves and does not affect optical surface precision for high groove density gratings with a groove depth of 10 nm or so [13]. However, the optical surface of an ultra-precise substrate can degrade during the wet etching for coarse blazed gratings with a groove depth of hundreds of nanometers. Since a substantial surface layer as thick as 1 micron is removed during the etching, even a tiny non-uniformity of the etching may cause significant degradation of the surface average planarity. The suggested fabrication method provides a way to recover the surface precision during the blaze angle reduction process. On the other hand, the LBA substrate undergoes minimal processing by the plasma etch which removes a surface layer as thin as the final groove depth, i.e. typically a few tens of nanometers, and the risk of optical surface degradation due to the plasma etch non-uniformity is negligible.

In this work we achieved a global substrate surface change as small as 10 nm p/v for the blaze angle reduction process. The introduced surface errors are acceptable for many applications but for ultimate x-ray optics applications the errors should be further reduced. For example, residual surface errors should not exceed 1 nm p/v for coherent x-ray optics [1]. There are two possibilities to improve the surface of the final grating. First, the nanoimprint step should be improved to achieve better resist layer uniformity. Second, one could use a higher reduction factor to scale down the imperfections to a higher degree. In this case the master would have a larger blaze angle (which could be easily increased up to 6 degrees [20]) and the plasma etch recipe would be modified accordingly.

The reduction process offers a valuable extension to the wet etching process and gives flexibility in blaze angle modification or correction. For example, two or more gratings with different blaze angles can be made on the same substrate which is not possible using the anisotropic etching only.

4. Summary

We developed a new process for low blaze angle x-ray gratings based on nanoimprint replication of a large blaze angle master followed by a plasma etch of the resist replica, which provides transfer of the saw-tooth grooves into a Si grating substrate. The reduction of the blaze angle is achieved owing to the difference in etch rates of the resist and Si. The method is highly reproducible and provides high accuracy for the low blaze angles. The process preserves an ideal shape of the saw-tooth grooves and high precision of the optical surface of the grating substrate. The reduction process results in improvement of the grating quality by suppression of the imperfections of the master grating such as facet curvature, surface roughness etc. The fabricated low blaze angle grating prototypes exhibited diffraction efficiency up to 35.8% which is almost as high as the theoretical efficiency of 37.7%. The method offers great flexibility in the post fabrication modification of blaze angles and demonstrates blaze angle reduction down to the extremely small values required for soft, tender and even hard x-ray applications.

Acknowledgements. The Advanced Light Source and the Molecular Foundry are supported by the Director, Office of Science, Office of Basic Energy Sciences, of the U.S. Department of Energy under Contract No. DE-AC02-05CH11231.

Disclaimer. This document was prepared as an account of work sponsored by the United States Government. While this document is believed to contain correct information, neither the United States Government nor any agency thereof, nor The Regents of the University of California, nor any of their employees, makes any warranty, express or implied, or assumes any legal responsibility for the accuracy, completeness, or usefulness of any information, apparatus, product, or process disclosed, or represents that its use would not infringe privately owned rights. Reference herein to any specific commercial product, process, or service by its trade name, trademark, manufacturer, or otherwise, does not necessarily constitute or imply its endorsement, recommendation, or favoring by the United States Government or any agency thereof, or The Regents of the University of California. The views and opinions of authors expressed herein do not necessarily state or reflect those of the United States Government or any agency thereof or The Regents of the University of California.

Disclosures. The authors declare no conflicts of interest.

Data availability. Data underlying the results presented in this paper are not publicly available at this time but may be obtained from the authors upon reasonable request.

References

1. D. Cocco, G. Cutler, M. Sanchez del Rio, L. Rebuffi, X. Shi, and K. Yamauchi, "Wavefront preserving X-ray optics for Synchrotron and Free Electron Laser photon beam transport systems," *Phys. Reports* **974**, 1–40 (2022).
2. <https://www.inprentus.com/technology>.
3. <https://als.lbl.gov/als-u/als-u-project-beamlines/>.
4. J. Gao, P. Chen, L. Wu, B. Yu, and L. Qian, "A review on fabrication of blazed gratings," *J. Phys. D: Appl. Phys.* **54**(31), 313001 (2021).
5. B. Nelles, K.F. Heidemann, and B. Kleemann, "Design, manufacturing and testing of gratings for synchrotron radiation," *NIMA* **467-468**, 260–266 (2001).
6. D. L. Voronov, P. Lum, P. Naulleau, E. M. Gullikson, A. V. Fedorov, and H. A. Padmore, "X-ray diffraction gratings: precise control of ultra-low blaze angle via anisotropic wet etch," *Appl. Phys. Lett.* **109**(4), 043112 (2016).
7. D. Cocco, A. Bianco, B. Kaulich, F. Schaefers, M. Mertin, G. Reichardt, B. Nelles, and K. F. Heidemann, "From Soft to Hard X-ray with a Single Grating Monochromator," *AIP Conf. Proc.* **879**, 497–500 (2007).
8. D. L. Voronov, E. M. Gullikson, and H. A. Padmore, "Ultra-low blaze angle gratings for synchrotron and Free Electron Laser applications," *Opt. Express* **26**(17), 22011–22018 (2018).
9. D. L. Voronov, S. Park, E. M. Gullikson, F. Salmassi, and H. A. Padmore, "Highly efficient ultra-low blaze angle multilayer grating," *Opt. Express* **20**(11), 16676–16685 (2021).
10. S. Park, D. L. Voronov, A. Wojdyla, E. M. Gullikson, F. Salmassi, and H. A. Padmore, "Fabrication of low blaze angle gratings by replication and plasma etch," *Proc. SPIE* **12240**, 13 (2022).
11. Y. Fujii, K. I. Aoyama, and J. I. Minowa, "Optical demultiplexer using a silicon echelle grating," *IEEE J. Quantum Electron.* **16**(2), 165–169 (1980).
12. P. Philippe, S. Valette, O. M. Mendez, and D. Maystre, "Wavelength demultiplexer: using echelle gratings on silicon substrate," *Appl. Opt.* **24**(7), 1006–1011 (1985).
13. D. L. Voronov, S. Park, E. M. Gullikson, F. Salmassi, and H. A. Padmore, "6000 lines/mm blazed grating for a high-resolution x-ray spectrometer," *Opt. Express* **30**(16), 28783–28794 (2022).
14. A. J. Nijdam, J. G. E. Gardeniers, C. Gui, and M. Elwenspoek, "Etching pits and dislocations in Si {111},," *Sens. Actuators, A* **86**(3), 238–247 (2000).
15. <https://www.microresist.de/en/>.
16. H. Gao, H. Tan, W. Zhang, K. Morton, and S. Y. Chou, "Air cushion press for excellent uniformity, high yield, and fast nanoimprint across a 100 mm field," *Nano Lett.* **6**(11), 2438–2441 (2006).
17. <https://www.filmetrics.com/thickness-measurement/f20>.
18. Jean Paul Hugonin and Philippe Lalanne, "RETICOLO software for grating analysis," *arXiv*, arXiv:2101.00901 (2021).
19. <https://cxro.lbl.gov/reflectometer>.
20. D. L. Voronov, R. Cambie, E. M. Gullikson, V. V. Yashchuk, H. A. Padmore, Yu. P. Pershin, A. G. Ponomarenko, and V. V. Kondratenko, "Fabrication and characterization of a new high density Sc/Si. multilayer sliced grating," *Proc. SPIE* **7077**, 707708 (2008).